

Determination of fracture parameters of concrete interfaces using DIC

S. G. Shah & J. M. Chandra Kishen

Dept. of Civil Engineering, Indian Institute of Science, Bangalore 560012, India

ABSTRACT: The fracture properties such as mode I and mode II fracture toughness and the critical strain energy release rate for different concrete-concrete jointed interfaces are experimentally determined using Digital Image Correlation technique. Interface beam specimens having different compressive strength materials on either side of a centrally placed vertical interface are prepared and tested under three-point bending in a closed loop servo-controlled testing machine under crack mouth opening displacement control. Digital images are captured before loading (undeformed state) and at different instances of loading. These images are correlated and the surface displacements are computed from which the surface strains, crack opening displacements, load-point displacement, crack length and crack tip location are computed. It is seen that the CMOD and vertical load-point displacement computed using DIC analysis matches well with those measured experimentally. It is shown that the digital image correlation technique can be very useful for determination of fracture parameters.

1 INTRODUCTION

Currently, the research towards understanding of fracture behavior of bi-material interface has been a major area. Understanding the behavior of an interface formed between old and new concrete is very important in order to predict the performance of a repaired structure. In composite structures and materials, the weakest part is often the interface between different materials (Walter et al. 2005). An interface appears when a repair material is applied to an infrastructure system after rehabilitation. Usually the interface is relatively weaker than the material on either side of it, in a repaired system. The performance of the repaired system under loading is strongly dependent on the performance of the interface. Compatibility between repair material and substrate concrete is recognized to be important for prevention of cracking but reliable quantification of the required parameters is lacking (Mangat & O'Flaherty 2000). Further, in order to protect concrete constructions, quite often layers of concrete or cement bonded materials are used thereby forming an interface (Tschegg & Stanzl 1991). The bonding at interfaces in concrete structures is important for safety and durability (Kunieda et al. 2000). The chances of failure by cracking along the interface are higher because of stress concentration and rapid change of stress levels along the interface.

Concrete is a heterogeneous material, wherein its fracture behavior is complicated and the quantification of fracture parameters becomes difficult. To obtain microscopic information on the failure processes in concrete, a robust full-field measurement method is required (Choi & Shah 1997). Direct observation of the fracture process is difficult because of the small scale at

which the micro-structural features interact with the failure process. A more robust method for studying the fracture processes is the Digital Image Correlation (DIC), which has been successfully applied to detect cracks in concrete and other materials. Using DIC, full-field surface displacements can be measured with high accuracy for specimens with multiple cracks at incremented levels of fracture. This technique can be used to monitor the testing of a wide range of specimen sizes under different loading conditions (Lawler & Shah 2002).

Only a few experimental works have been reported regarding the behavior of an interface between old and new concrete. Tschegg and Stanzl (Tschegg & Stanzl 1991) have measured the adhesive power of bond between old and new concrete by means of a cubic specimen with a rectangular groove and a starter notch was split by wedge-load equipment at the interface of two materials. Tschegg and co-workers (Tschegg et al. 1993) have introduced interfaces with high and low adhesion between old and new concrete for studying their fracture behavior. Kunieda and co-workers (Kunieda et al. 2000) have evaluated the bond properties at the interface between old and new concrete using the tension softening diagrams. Chandra Kishen and Rao (Chandra Kishen & Rao 2007) have experimentally investigated the fracture behavior of concrete-concrete transverse jointed interface specimens.

However, not much work has been reported in the literature on the determination of fracture properties, such as the mode I and mode II fracture toughness and fracture energy for concrete-concrete interfaces. These properties are required in linear and non-linear fracture mechanics based finite element analysis of structures having joints and interfaces. Proper characterization of the interfaces is necessary for

performing failure and cracking analysis of structures having interfaces and joints especially, in the case of patch repaired concrete structures which use concrete overlays, repaired concrete pavements, cold joints in mass concrete structures (dams) etc.

In this paper, DIC technique is employed for measuring surface displacements and crack lengths in concrete-concrete interface specimens, which are further used for computation of fracture properties such as mode I and mode II fracture toughness and critical energy release rate.

2 DIGITAL IMAGE CORRELATION

Digital image correlation (DIC) is an optical and non-contact measurement technique and is adopted to analyze the displacements on the surface of an object of interest. In digital image correlation, the surface images before and after the deformation are taken by a digital camera from which the displacement at any point of the image is computed. DIC is extensively used to study a very large range of materials, in widely different range of scales. Originally developed in the eighties (Sutton et al. 1983, 1986) the DIC-based methods and their fields of application have been growing steadily due to the technological progress and affordability of digital imaging systems. DIC is based on the following principles: the image of the body is described by a discrete function representing the grey level of each pixel. The grey level is a value between 0 and 255 of its grey levels with the lowest value representing black, highest value white, and values in between representing different shades of gray. The correlation calculations are carried out for a set of pixels, called a pattern. The displacement field is assumed to be homogeneous inside a pattern. The initial image representing the body before distortion is a discrete function $f(x, y)$ and is transformed into another discrete function $f^*(x^*, y^*)$ after distortion or displacement. The theoretical relation between the two discrete functions can be written as (Touchal et al. 1997):

$$f^*(x^*, y^*) - f(x + u(x, y), y + v(x, y)) = 0 \quad (1)$$

where, $u(x, y)$ and $v(x, y)$ represent the displacement field for a pattern as shown in Figure 1.

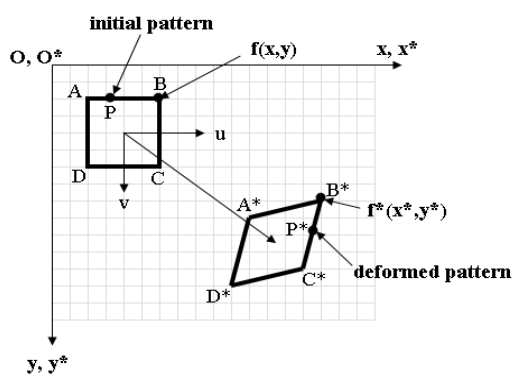


Figure 1. Initial and Deformed Pattern.

Image correlation now becomes a job of comparing subsets of numbers between the two digital images. A typical cross correlation coefficient which measures how well subsets match is given by

$$C = 1 - \frac{\sum[f(x, y) \cdot f^*(x^*, y^*)]}{[\sum(f(x, y)^2) \cdot \sum(f^*(x^*, y^*)^2)]^{1/2}} \quad (2)$$

where $f(x, y)$ is the gray level value at coordinate (x, y) for initial image and $f^*(x^*, y^*)$ is the gray level value at point (x^*, y^*) of the deformed image. The coordinates (x, y) and (x^*, y^*) are related by the deformation which has occurred between acquisition of the two images. If the motion of the object relative to the camera is parallel to the image plane, then they are related by;

$$\begin{aligned} x^* &= x + u + \frac{\partial u}{\partial x} \Delta x + \frac{\partial u}{\partial y} \Delta y \\ y^* &= y + v + \frac{\partial v}{\partial x} \Delta x + \frac{\partial v}{\partial y} \Delta y \end{aligned} \quad (3)$$

where u and v are the displacements for the subset centers in the x and y directions, respectively. The terms Δx and Δy are the distances from the subset center to point (x, y) . By performing image correlation, the values of coordinates (x, y) , displacement (u, v) , and their derivatives can be determined (Touchal et al. 1997, Bruck et al. 1989). These are in turn used for further analysis, for example, in the computation of fracture parameters.

3 FRACTURE AT BI-MATERIAL INTERFACE

Unlike fracture in homogeneous materials wherein the mode I and mode II stress intensity factors are functions of the normal and shear stresses respectively, fracture of crack between a bi-material interface is mixed-mode even though the geometry is symmetric with respect to the crack and loading is either of pure mode I or mode II. The stress intensity factors in mode I and mode II represented by K_1 and K_2 respectively, are functions of both the normal and shear stress.

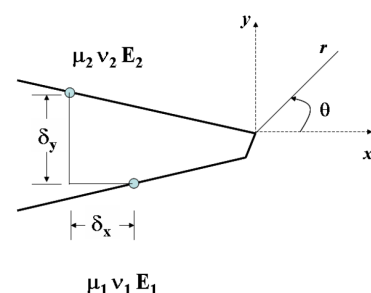


Figure 2. Crack at Bi-material Interface.

The crack flank displacement at a distance r (Fig. 2) from the crack tip for plane strain is given by (Smelser 1979, Carlsson & Prasad 1993):

$$\delta_x + i\delta_y = \frac{4}{\sqrt{2\pi}} \frac{(\frac{1}{E_1} + \frac{1}{E_2})(K_1 + iK_2)}{(1 + 2i\varepsilon)\cosh(\pi\varepsilon)} \sqrt{rr}^{i\varepsilon} \quad (4)$$

where, E_1 and E_2 are elastic modulus of material 1 and 2 on either side of the interface, respectively. K_1 and K_2 are opening and sliding mode stress intensity factors and x and y are the opening and sliding displacements of two initially coincident points on the crack surfaces behind the crack tip, respectively. ε is a bi-material parameter known as an oscillatory index and is defined by

$$\varepsilon = \frac{1}{2\pi} \ln \left[\frac{1 - \beta}{1 + \beta} \right] \quad (5)$$

where β is one of Dunder's elastic mismatch parameters (Dunders 1969), which for plane strain is given by:

$$\beta = \frac{\mu_1(1 - 2\nu_2) - \mu_2(1 - 2\nu_1)}{2[\mu_1(1 - \nu_2) + \mu_2(1 - \nu_1)]} \quad (6)$$

where μ , ν and a are the shear modulus, Poisson's ratio and crack length, respectively, and subscripts 1 and 2 refer to the materials above and below the interface, respectively (Touchal et al. 1997, Bruck et al. 1989, Rethore et al. 2005). We note that both β and ε vanish when the materials above and below the interface are identical. The relation between crack flank displacement and stress intensity factor given in Equation 4 can be further solved to obtain the expression for mode-I and mode-II stress intensity factors as:

$$K_1 = \sqrt{\frac{2\pi}{r}} \frac{\cosh(\pi\varepsilon)}{4(\frac{1}{E_1} + \frac{1}{E_2})} [(\delta_x - 2\varepsilon\delta_y)\cos(\varepsilon\log_e r) + (\delta_y + 2\varepsilon\delta_x)\sin(\varepsilon\log_e r)] \quad (7)$$

$$K_2 = \sqrt{\frac{2\pi}{r}} \frac{\cosh(\pi\varepsilon)}{4(\frac{1}{E_1} + \frac{1}{E_2})} [(\delta_y + 2\varepsilon\delta_x)\cos(\varepsilon\log_e r) - (\delta_x - 2\varepsilon\delta_y)\sin(\varepsilon\log_e r)] \quad (8)$$

The above Equation are used for computing the bi-material stress intensity factors for the interface specimen by knowing the displacements. The energy release rate, G , for extension of the crack along the interface for plane strain is given by (Smelser 1979, Carlsson & Prasad 1993):

$$G = \frac{(\frac{1}{E_1} + \frac{1}{E_2})(K_1^2 + K_2^2)}{2\cosh^2(\pi\varepsilon)} \quad (9)$$

4 EXPERIMENTAL PROGRAM

The experimental program consists of preparation and testing of interface specimens. The interface specimens are prepared using standard Portland cement having specific gravity of 3.15, river sand passing through 4.75 mm sieve, having specific gravity and fineness modulus of 2.67 and 2.37, respectively and crushed granite stones having maximum size of 12 mm and specific gravity of 2.78. The dimensions of the specimens are 810 mm length, 304 mm depth and 50 mm thickness as shown in Figure 3.

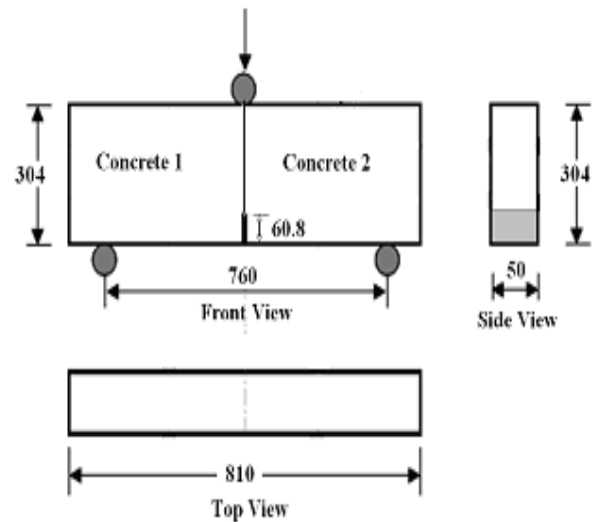


Figure 3. Details of specimen geometry.

The specimens having a span of 760 mm are tested under three-point bending. All the beams are notched with an initial notch size (a_0) of 60.8 mm and notch width of 2 mm. Table 1 shows the mix proportions and elastic properties of the different mixes of concretes. The interface specimens are prepared as follows. On day one, the first-half of the beam is casted with mix A. On day two, the interface is cleaned with a water jet and is kept exposed for 24 hours. A notch is introduced at the interface during the casting process itself by inserting a wooden strip of 2 mm thickness. On day three, the second-half of the beam is casted by mixes A, B, C and D. This creates an interface between two mixes of concrete at the mid-span. On day four, the specimens are demoulded and kept in water for curing. While handling the specimens, great care is taken to prevent falling or impact. The designation of the beams with and without the interface is given in Table 2.

Table 1. Details of materials & mix proportions.

No.	Mix	Cement	Mix	Comp.	Elastic	Poisson's
		Quantity (kg/m ³)	Proportion C : FA : CA : w/c	Strength (MPa)	Modulus (GPa)	Ratio
1	A	385.2	1 : 1.86 : 2.61 : 0.54	34	30	0.20
2	B	495.2	1 : 1.22 : 2.03 : 0.42	45	32	0.19
3	C	547.4	1 : 1.01 : 1.83 : 0.38	54	34	0.19
4	D	650.0	1 : 0.69 : 1.54 : 0.32	66	35	0.19

Table 2. Designation of interface beams.

No.	Specimen Designation	Description
1	AI	No interface. Intact beam of mix A
2	AA	Interface between mixes A and A
3	AB	Interface between mixes A and B
4	AC	Interface between mixes A and C
5	AD	Interface between mixes A and D

Intact beams (AI) without any interface are also casted to compare its behavior with the beams having an interface. The interface specimens are tested in a closed loop servo-controlled testing machine having a capacity of 500 kN. A specially calibrated 50 kN load cell is used for measuring the load. The load-point displacement is measured using a linear variable displacement transformer (LVDT). The CMOD is measured using a clip gage located across the notch. All the tests are performed under CMOD control with the rate of crack opening being 0.0005 mm/sec. The results of load, vertical displacement, CMOD and time are simultaneously acquired through a data acquisition system. For digital image correlation, the speckle pattern is to be made on the specimen. The specimens are initially white washed and a speckle pattern is prepared over it using a standard black spray paint. The images of the interface specimen are captured before loading and during various stages of loading using a digital camera mounted on a stand as shown in Figure 4. A remote control is used for capturing the images to avoid any vibration and also to keep the distance between camera lens and the specimen unchanged.

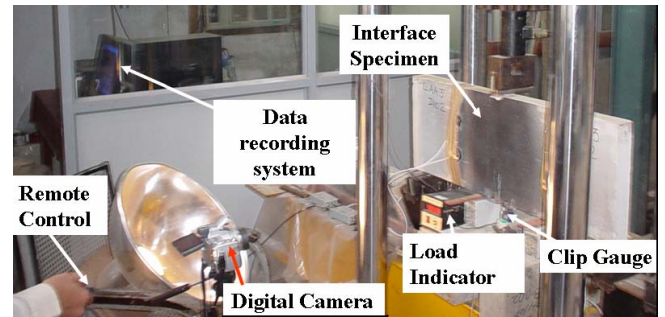


Figure 4. Experimental set-up.

5 RESULTS AND DISCUSSIONS

The digital images taken during the experiments for all the specimens are correlated using a code (Eberl 2006) written within the framework of mathematical package MATLAB. The results obtained from the DIC analysis of interface beams at different stages of loading are presented and discussed. A square grid pattern of 5 pixels in each of x and y directions are selected such that the interface falls within the center of grid as shown in Figure 5, which is used for further analysis.

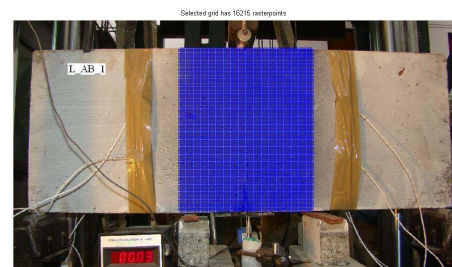


Figure 5. Grid Pattern used for DIC analysis.

5.1 Surface displacements & strains

DIC analysis provides the surface displacements of the each point of the speckle pattern. Figures 6-8 shows the surface displacements and strains obtained from DIC analysis for selected images. These figures show how the pattern of crack propagation under different stages of loading. The images shown in Figure 6 are used for calculation of crack length and crack tip locations and used for quantifying the crack opening displacement which is discussed later on.

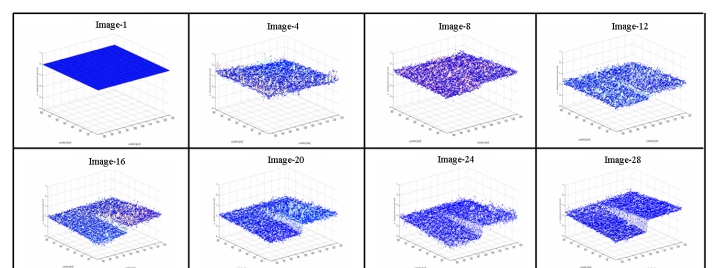


Figure 6. Displacement and cracking pattern obtained from DIC (selected images).

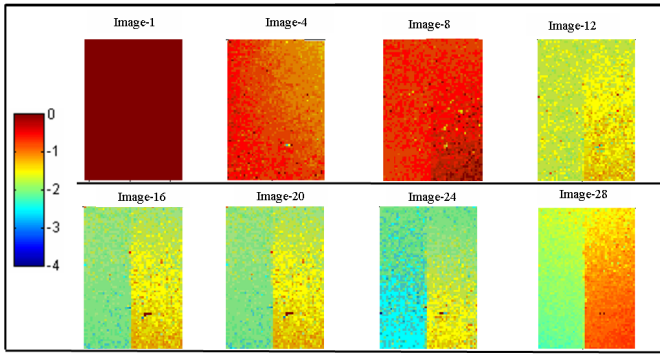


Figure 7. Surface displacement from DIC (selected images).

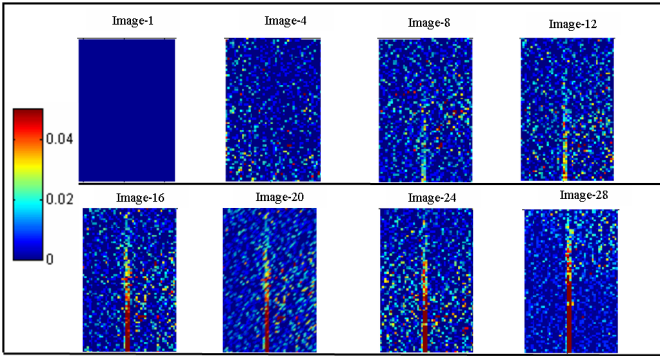


Figure 8. Surface strains from DIC (selected images).

5.2 Crack length

The method employed for determining crack opening displacement (δ_x), crack tip location and the distance of crack tip (r) from the digitally processed images is shown in Figure 9.

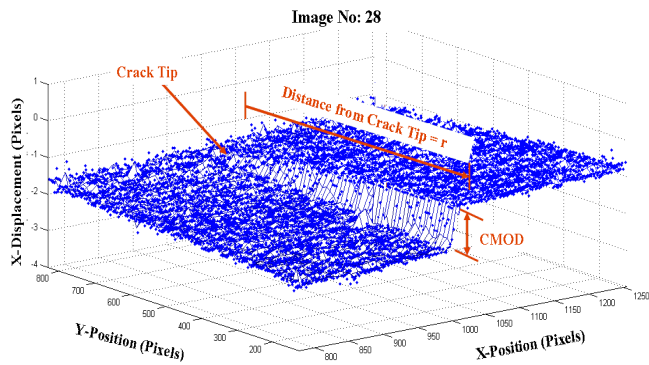


Figure 9. Crack tip and CMOD measurement from DIC.

The crack lengths are computed for all the images and are plotted against load as shown in Figure 10. From this figure, it can be seen that the crack has not propagated until the loading stage corresponding to image number four. The load corresponding to image four is about 85 to 90 % of the peak load. It is also seen that there is a departure from linearity at 85 to 90% of peak load. This is due to the development of micro-cracks in the fracture process zone that forms ahead of the traction free crack which is a property of quasi-brittle material.

According to the theory of linear elastic fracture mechanics, we use the concept of effective elastic crack length, defined as the crack length that is longer than

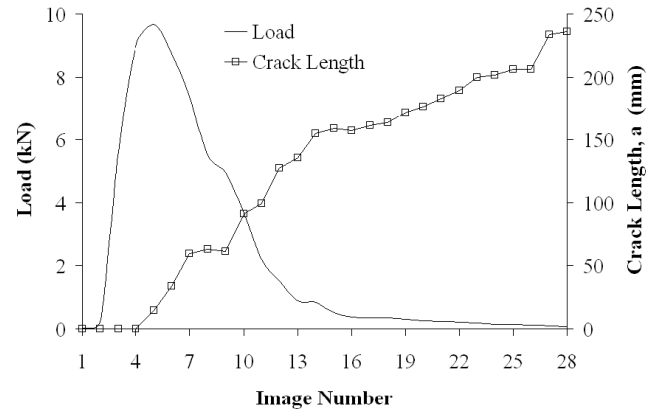


Figure 10. Load versus crack length.

the true crack but shorter than true crack plus the fracture process zone as shown in Figure 11, and define critical crack length as the crack length corresponding to peak load as shown in Figure 10.

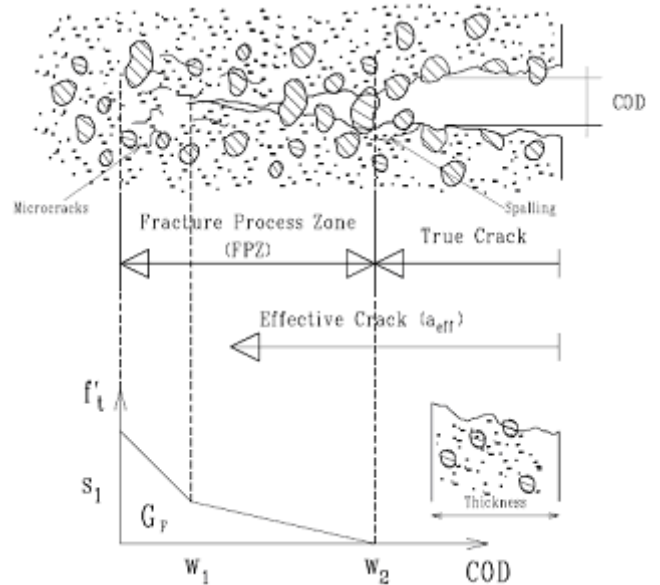


Figure 11. Concept of effective crack length.

Furthermore, the properties that are required for linear elastic fracture mechanics analysis are computed at this critical crack length. The critical crack lengths obtained for different interface specimens are listed in Table 3. It is seen that as the difference between the compressive strength of the concrete on either side of the interface increases, the critical length decreases, which shows the increase in the brittleness of the interface specimens which have higher mismatch of property on either side of the interface. This feature of obtaining the crack tip location and determination of crack length makes the DIC technique very attractive as it is very difficult to obtain these parameters through other methods. Techniques such as dye penetration for determination of the crack length have been reported in the literature and are difficult in terms of usage in addition to being expensive too.

Table 3. Critical crack lengths computed from DIC.

Sr. No.	Specimen Designation	Critical Crack Length (mm)
1	AI	16.92
2	AA	15.95
3	AB	14.79
4	AC	8.50
5	AD	4.76

5.3 Crack mouth opening displacement

The advantage of DIC technique is that we can determine the crack opening displacement at any position along the crack as shown in the Figure 9, which is not possible with other experimental sensors such as, a clip gage, unless we mount a number of them along the crack.

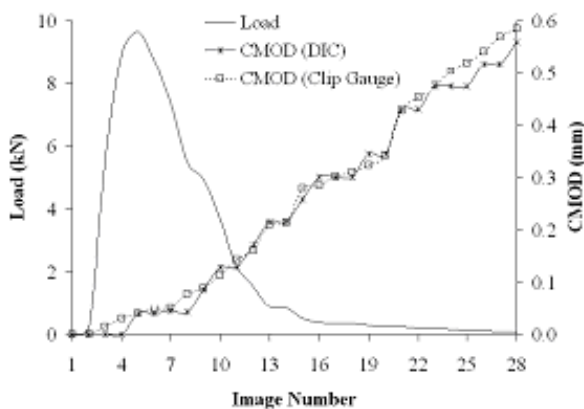


Figure 12. Load versus CMOD.

For validation of the results obtained from DIC, the CMOD computed for all the images using DIC analysis are plotted and compared with those measured experimentally using clip gage, as shown in Figure 12. It is seen that there is a very close match between the two. However, one drawback of DIC analysis seen is that the measurement of CMOD during the initial loading portion is difficult since the crack does not get initiated as seen from the results of images 1 to 4.

5.4 Fracture properties of concrete interfaces

The mode I and mode II fracture toughness of the interface beams are determined by substituting the values of crack opening displacement (δ_x) and crack sliding displacement (δ_y) computed at the critical crack length position in to Equations 7 and 8, respectively.

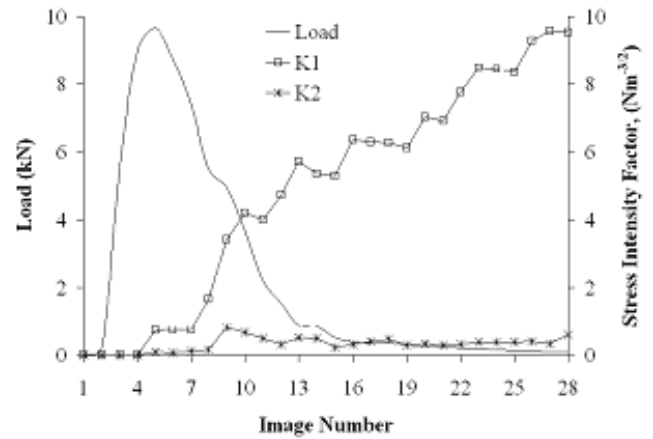


Figure 13. Load versus stress intensity factors.

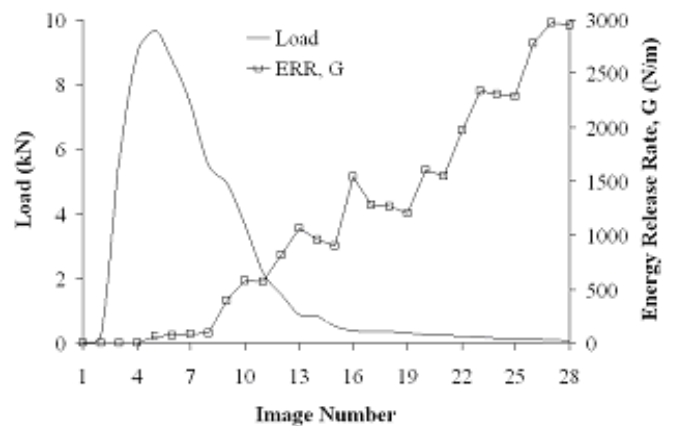


Figure 14. Load versus energy release rate.

Since, the fracture toughness are linear elastic fracture mechanics parameters, these are obtained at the critical crack length which in this work is assumed to have occurred at the maximum load level. Figure 13 shows the plot of mode-I and mode II stress intensity factors computes from DIC for different images. The mode I fracture toughness (K_{IC}) computed for different interfaces are shown in Table 4. The values obtained by using the Rilem method (RILEM 1990) which is based on the size effect law of Bazant (Bazant 1984) are also shown in this table (Shah 2009). In addition, the values reported for different interfaces in Reference (Rao 2006) obtained using the compliance method are also shown. It is seen that the mode I fracture toughness computed using DIC agrees well with those obtained using the Rilem method. It may be noted that the Rilem method requires only the maximum loads obtained for geometrically similar specimens of different sizes and the modulus of elasticity.

The values of mode II fracture toughness computed for different interfaces are reported in Table 5. For comparison the values reported in Reference (Rao 2006) are also shown. The values reported in Reference (Rao 2006) are for interfaces with concrete strength different from

Table 4. Comparison of K_{Ic} Values.

Specimen	K_{Ic} (MPa \sqrt{m})		
	Designation	DIC	Rao 2006
AI	1.39	1.15	1.37
AA	0.86	0.89	1.13
AB	0.73	0.76	1.05
AC	0.64	0.71	0.93
AD	0.55	0.62	0.75

Table 5. Comparison of K_{IIc} Values.

Specimen	K_{2c} (MPa \sqrt{m})	
	Designation	Rao 2006
AI	NA	NA
AA	0.01	0.00
AB	0.08	0.07
AC	0.10	0.09
AD	0.18	0.17

the ones used in this study. It is provided here only for the sake of comparing the range in which the results fall. It may be noted here that due to the difference in the elastic properties of concrete on either side of the interface, mode II component is present although the shear stress along the interface is negligible. Only mode I values of fracture toughness can be obtained using the Rilem method since it is derived for single homogeneous material. Hence, the mode II fracture toughness using the Rilem method is not reported in Table 5.

Table 6. Comparison of G_C Values.

Specimen	G_C (N/m)		
	Designation	DIC	Rao 2006
AI	119.67	166.71	108.85
AA	95.32	123.98	87.50
AB	66.08	96.16	82.29
AC	43.45	86.81	74.90
AD	18.10	59.17	72.68

The energy release rate, G which is defined as the energy required for creating a crack of unit area, is

computed by substituting values of K_{Ic} and K_{IIc} in Equation 9. Figure 14 shows the plot of energy release rate versus load for different images. Table 6 shows the energy release rate values computed for different interfaces. The values obtained from Reference (Rao 2006) are also shown for the sake of comparing the value under which the present results fall.

6 CONCLUSIONS

The bi-material fracture toughness in mode I (K_{Ic}) and mode II (K_{IIc}) and the critical energy release rate (G_c) are experimentally determined for a concrete-concrete jointed interface specimen using digital image correlation technique. The concrete-concrete interface specimens are tested under three point bending in a closed loop servo-controlled testing machine under crack mouth opening displacement control. The images of the interface specimen are captured during various stages of loading using a digital camera. Using correlation methods, the images are analyzed and the surface displacements, surface strains, crack mouth opening displacement, crack sliding displacement and crack length are computed. It is seen that there is very good agreement in the vertical displacements and crack mouth opening displacements computed through DIC and those measured using LVDT and clip gage, respectively. It can be concluded that the simple DIC technique can be a very useful and an economical substitute against strain gages, clip gages and LVDTs. Further, the measurement of crack tip location and crack length can be done effectively using DIC techniques which are very difficult and expensive for concrete like materials using traditional sensors.

REFERENCES

- Bazant Z. P. 1984. Size effect in blunt fracture: Concrete, rock, metal. *Journal of Engineering Mechanics* 110: 518–535.
- Bruck H. A., McNeill S. R., Sutton M. A. & Peters W. H. 1989. Digital image correlation using Newton-Raphson method of partial differential correction. *Experimental Mechanics* 29: 261–267.
- Carlsson L. A. & Prasad S. 1993. Interfacial fracture of sandwich beams. *Engineering Fracture Mechanics* 44: 581–590.
- Chandra Kishen J. M. & Rao P. S. 2007. Fracture of cold jointed concrete interfaces. *Engineering Fracture Mechanics* 74: 122–131.
- Choi S. & Shah S. P. 1997. Measurement of deformations on concrete subjected to compression using image correlation. *Experimental Mechanics* 37: 307–313.
- Dunders J. 1969. Edge-bonded dissimilar orthogonal elastic wedges under normal and shear loading. *Journal of Applied Mechanics* 36: 650–652.
- Eberl C. 2006. Digital Image Correlation and Tracking. <http://www.mathworks.com/matlabcentral/fileexchange/12413>.
- Kunieda M, Kurihara N, Uchida Y & Rokugo K 2000. Application of tension softening diagrams to evaluation of bond

- properties at concrete interfaces. *Engineering Fracture Mechanics* 65: 299–315.
- Lawler J. S. & Shah S. P. 2002. Fracture processes of quasi-brittle materials studied with digital image correlation. In: *Recent Advances in Experimental Mechanics*. Kluwer Academic Publishers, Netherlands, pp. 335–344.
- Mangat P. & O'Flaherty F. 2000. Influence of elastic modulus on stress redistribution and cracking in repair patches. *Cement & Concrete Research* 30: 125–136.
- Rao P. S. 2006. *Fracture behavior of jointed concrete interfaces*. Ph.D. thesis, Department of Civil Engineering, Indian Institute of Science, Bangalore, India.
- Rethore J., Gravouil A., Morestin F. and Combescure A. 2005. Estimation of mixed-mode stress intensity factors using digital image correlation and an interaction integral. *International Journal of Fracture* 132: 65–79.
- RILEM draft recommendations. 1990. Size-effect method for determining fracture energy and process zone size of concrete. *Material & Structures* 23: 461–465.
- Shah S. G. 2009. *Fracture & fatigue behavior of concrete-concrete interfaces using acoustic emission, digital image correlation and micro-indentation techniques*. Ph.D. thesis, Department of Civil Engineering, Indian Institute of Science, Bangalore, India.
- Smelser R. E. 1979. Evaluation of stress intensity factors for biomaterial bodies using numerical crack flank displacement data. *International Journal of Fracture* 15: 135–143.
- Sutton M. A., Cheng M., Peters W.H., Chao Y.J. & McNeill S.R. 1986. Application of an optimized digital correlation method to planar deformation analysis. *Image and Vision Computing* 4: 143–150.
- Sutton M. A., Wolters W. J., Peters W. H., Ranson W. F. & McNeill S. R. 1983. Determination of displacements using an improved digital correlation method. *Image and Vision Computing* 1: 133–139.
- Touchal S.M., Morestin F. & Brunet M. 1997. Various experimental applications of digital image correlation method. In: *Proceedings of International conference on computational methods and experimental measurements*. Rhodes, Greece, pp. 45–58.
- Tschegg E. K. & Stanzl S. E. 1991. Adhesive power measurement of bonds between old and new concrete. *Journal of Material Science* 26: 5189–5194.
- Tschegg E. K., Tan D. M., Kirchner H. O. K. & Stanzl S. E. 1993. Interfacial and subinterfacial fracture in concrete. *Acta metallurgical materials* 41: 569–576.
- Walter R., Ostergaard L., Olesen J. F. & Stang H. 2005. Wedge splitting test for a steel-concrete interface. *Engineering Fracture Mechanics* 72: 2565–2583.